A High-Speed, High-Frequency, Air-Core PM Machine for Aircraft Application

Andy Yoon, Xuan Yi, Jon Martin, Yuanshan Chen, Kiruba Haran
School of Electrical and Computer Engineering
University of Illinois at Urbana-Champaign
Email: yoon62@illinois.edu

***Abstract*—High number of magnetic poles in an electric machine allows reduction in radial thickness of stator and rotor yoke and thus heavy alloy. If frequency is allowed to increase with pole-count (constant speed), power level can be maintained. Thus, high frequency, together with high pole count, can improve power density of rotating electric machines. The proposed high frequency concept is applied to designing a 1 MW motor, with power density and efficiency goals of $> 13kW/kg$ and $> 96\%$, respectively .**

***Index Terms*—AC machines, air core, high pole count, Halbach arrays, air gap winding, high speed, high frequency, outer rotor.**

1. Introduction

According to the International Air Transport Association (IATA), 2.4 billion passengers and 40 million tons of goods were transported in 2010. IATA also estimates that, by 2050, the industry will transport sixteen billion passengers and 400 million tons of goods [1]. Financial and environmental concerns due to the projected increase in air-traffic and thus jet fuel consumption are causing the aviation industry to turn towards turbo-electric propulsion technology. This technology uses energy-dense fossil fuel instead of batteries as a power source for the electric generators, because of relatively low energy density of batteries and air vehicles' sensitivity to weight. Also, electric motors replace jet engines for propulsion, which has multiple advantages in addition to high fuel efficiency [2]. Thus, National Aeronautics and Space Administration (NASA) has identified a key enabling technology of turbo-electric propulsion system as electric motors with four times the power density of the current state-of-the-art (SOA) [3]. This paper proposes a motor to meet NASA's power, power density, and efficiency goals of 1MW, $> 13kW/kg$ and $> 96\%$, respectively, by minimizing the weight of the motor while maximizing the power output. Section 2.1 discusses the adoption of high-pole and high-frequency, air-gap windings, and Halbach arrays to enable an air-core topology. Section 2.2 discusses the use of Litz wire and outer-rotor assembly to address challenges in high-speed operation. Section 3 addresses the optimization efforts to finalize the design. Section 4 summarizes the design's key specs, loss breakdown, and weight breakdown.

2. Design Concept

2.1. Air-core Topology

The first approach to increase power density, which refers to the *amount of power per unit weight*, is to move away from the traditional metal-intense motor topology. High pole count in an electric machine allows both a thinner stator and rotor yoke due to less flux per pole, which is given by

$$\phi_p = \frac{2}{P} L_{stack} D B_{peak,ag} \tag{1}$$

where P, L_{stack}, D, and $B_{peak,ag}$ are number of poles, stack length, air-gap diameter, and peak flux density in the air-gap [4]. The opportunity to decrease the motor weight is clear, as doubling the pole count in a machine can reduce the yoke thicknesses by half. Furthermore, the power level can be maintained with reducing the weight if the frequency is allowed to increase with the pole-count, as rated power of a 3-phase AC machine is given as

$$P_{rated} = 3 E_{rms} I_{q,rms} \tag{2}$$

where E_{rms} and $I_{q,rms}$ refer to induced voltage and quadrature-axis component of the stator current, respectively, and induced voltage, or back-EMF, is given by

$$E_a = K_w N_{ph} \omega_e \phi_p sin(\omega_e t) \tag{3}$$

where K_w, N_{ph}, ω_e, and ϕ_p refer to winding factor, number of turns per phase, electrical frequency, and flux per pole, respectively. Challenges exist with the adoption of high pole count and high frequency. In addtion to the apparently high copper losses and iron-loss density, the magnetizing inductance for high-pole machines is reduced. So, machine types such as induction machines or reluctance machines can be incompatible with high-pole count, high-frequency topology. Permanent magnet synchronous machine (PMSM) or wound-rotor synchronous machines have separate excitation for rotor and stator. Thus, their performance is not directly affected by low magnetizing reactance. Figure 1 gives the FEA model built for preliminary analysis. Tab;e 1 gives the results, where an increase in power density is observed with increasing pole count and frequency for a PMSM.

978-1-5090-0261-0/16/$31.00 ©2016 IEEE

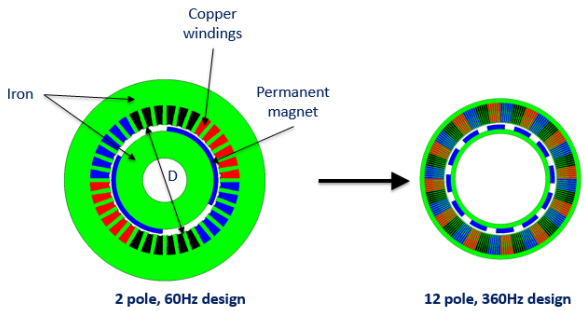

Figure 1. 2D EM FEA Model for 2-pole and 12-pole Motor

TABLE 1. PRELIMINARY FEA RESULTS FOR HIGH-POLE COUNT, HIGH-FREQUENCY TOPOLOGY

-	2pole	4pole	12pole
Frequency [Hz]	60	120	360
Stator Outer Radius [mm]	90.9	79.3	71.6
Air-Gap Radius [mm]	48.3	48.3	48.3
Average Torque [Nm]	10.3	11.0	10.9
Total Iron Volume $[10^3 cm^3]$	13.3	7.6	3.69
Power Density [kW/kg]	0.41	0.68	1.07

Air-gap winding is a second key enabling technology for an air-core motor. Traditionally, the winding is fit inside a slot formed by the stator back yoke and the stator teeth. Air-gap winding allows for the stator teeth to be eliminated, as shown in Figure 2. Generally, the stator teeth are prone to saturation and have relatively higher flux density, which leads to high iron loss density. Thus, air-gap winding topology can significantly lower the risk of high iron losses due to high frequency, and reduce weight.

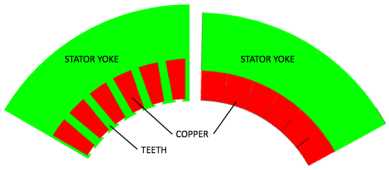

Figure 2. Demonstration of Air-Gap Winding

Finally, Halbach arrays are adopted to eliminate the rotor back yoke. Typically, magnets in a surface permanent magnet machines are oriented radially inward or outward to establish flux density in the air-gap. This requires a sufficient amount of iron to retain flux in the rotor back yoke. If the magnets are arranged in a Halbach array, the flux can be canceled on one side, thereby eliminating the heavy iron yoke [5]. In Figure 3, an example of Halbach array arrangement demonstrates the flux cancellation.

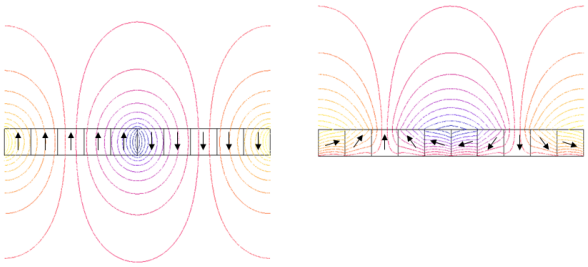

Figure 3. Conventional Magnet Arrangement Flux Lines(left) and Halbach Array Arrangement Flux Lines (right)

2.2. High-Speed Operation

The power level can be maintained with an increasing pole count if speed (proportional to ratio of frequency to pole-count) is kept constant. If the speed is allowed to increase, the power output can be increased. As increasing the speed affects iron/copper losses and the magnetic circuit, appropriate measures must be taken. Air-core topology allows a decrease in iron volume, making overall iron losses manageable, while high speed operation increases iron loss density due to high frequency. High frequency causes current density to be higher closer to the surface of the copper conductor carrying the alternating current. Consequently, the effective resistance grows, and the corresponding losses quadruple with frequency. The problem is addressed by employing Litz-wire, which divides each phase winding into high number of smaller-diameter conductors in parallel. The use of outer-rotor topology prevents the increase of effective air-gap caused by the increasing retaining ring thickness. Retaining rings are used in surface permanent magnet machines to keep magnets, affected by centrifugal force, from disassembling. With high speed, a substantial retaining ring thickness is required, which can reduce the air-gap flux density.

3. Design Optimization

Using traditional machine sizing equations, a baseline design of 3kHz, 10 pole-pair machine with outer diameter and active length of 12.2 inches and 15 inches, respectively, is chosen. The following sections describe efforts to optimize the machine dimensions.

3.1. Copper Depth Optimization

A detailed 2D electromagnetic-thermal FEA model was used to find the copper radial depth that will produce the maximum electrical loading. Because the allowable copper loss decreases with increasing copper radial depth due to greater winding thermal resistance, the allowable current density must also decrease. Copper losses were obtained for various copper radial depth from the thermal FEA model. Using results for dc and ac copper losses from baseline design, an iterative method was adopted to find allowable

current for each copper radial depth. The following assumptions were made: 1) Dc loss is inversely proportional to copper area and proportional to the square of the current; 2) Ac loss is proportional to the copper area and the square of the flux density. Figure 4 shows the relationship between

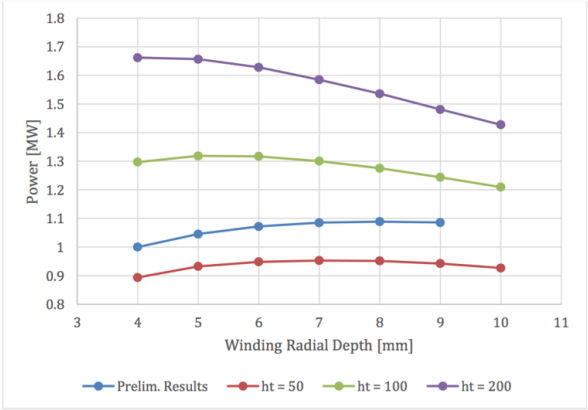

Figure 4. Power vs. Winding Radial Depth with Varying Heat Coefficients

winding radial depth and rated power with different heat transfer coefficients of the cooling channels. Using forced-air cooling and heat sinks on the inner diameter of the stator yoke, a heat-transfer coefficient of 100 W/m^2K is targeted. The optimal range of radial depth of copper is found to be between 5mm and 6mm.

3.2. Magnet and Stator Yoke Depth Optimization

To achieve the highest power density, 3D mechanical FEA model was used with a 2D EM FEA model to optimize the radial dimenstions of the magnet and the stator yoke. Using thicker magnets can shorten the active length, mitigating mechanical risks, such as excessive static deflection and rotor dynamic instability, inherent in cantilevered outer-rotor structures. But, the added radial weight increases the risk of air-gap radial expansion and thus air-gap reluctance. Note that the stator yoke thickness was also varied to include the effect of saturation in the yoke. Figure 5 shows the power density for various magnet and yoke radial dimensions. The optimum thickness of the magnet and stator yoke are 0.59 inch and 0.25 inch, respectively, with an active length of 8.4 inches.

3.3. Wire Gauge Size Optimization

Appropriate gauge size must be chosen to minimize copper losses while considering its effect on fill factor, number of strands, and manufacturability. Analytical method described in [6] is utilized to calculate total copper losses for different Litz wire strand sizes. Figure 6 shows the ac and dc losses for various strand sizes.

The results in Figure 6 indicate that decreasing the strand-diameter can minimize the total losses. However, other constraints on choosing the appropriate conductor

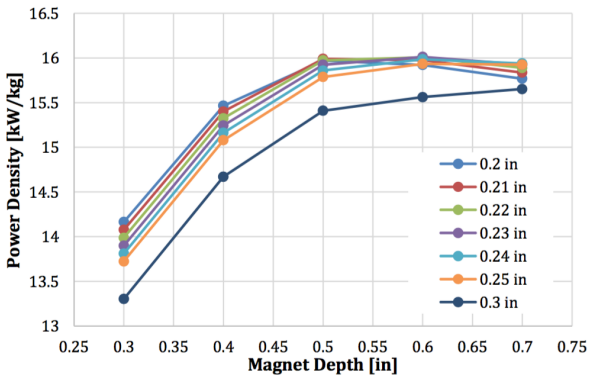

Figure 5. Power Density vs. Magnet Depth for Varying Yoke Depth

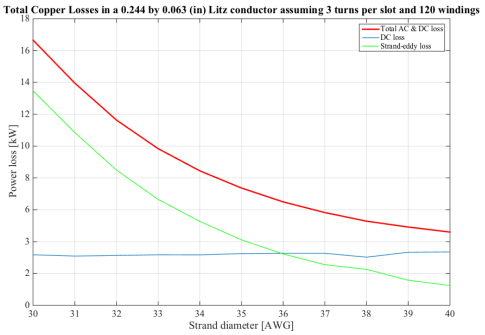

Figure 6. Analytical AC & DC Loss summary

must be considered. Firstly, a well-defined geometry of the Litz conductor is difficult to achieve at low strand diameters, which may increase the effect of eddy currents. Secondly, fill factor worsens with decreasing strand diameter because of inherent insulation thickness. Thus, a strand size of 38AWG, with total copper loss of 5.28kW, is employed upon trade-off analysis of total copper losses, fill factor, number of strands, and manufacturability. Figure 7 shows the 5/6 short pitch staggered winding for the proposed motor. It demonstrates the manufacturability challenges that exist with low-diameter strands for the end-windings, as the bends may experience greater force during operation and gap between the strands may increase during manufacturing.

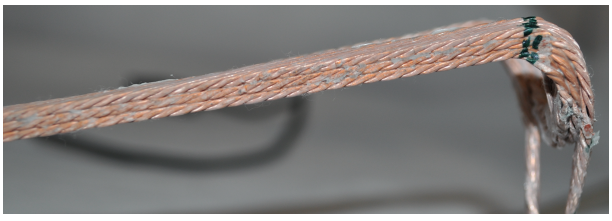

Figure 7. A Side-View of the End-Winding of a Coil Prototype

4. Final Design

Figure 8 shows the final design of the 1 MW motor. Table 2 summarize key specs of the proposed motor. Tables 3 and 4 summarize loss breakdown and weight breakdown, respectively, based on the finalized dimensions of the motor. Note that the overall magnet losses were calculated by observing the eddy currents in the magnet, using a 2D FEA model. Iron losses are calculated using modified Steinmetz coefficients found in [7], and windage losses were calculated using analytical methods found in [8] and [9]. Note that the range of windage losses, rather than a specific windage loss, is due to uncertainties regarding the operating environment of the motor.

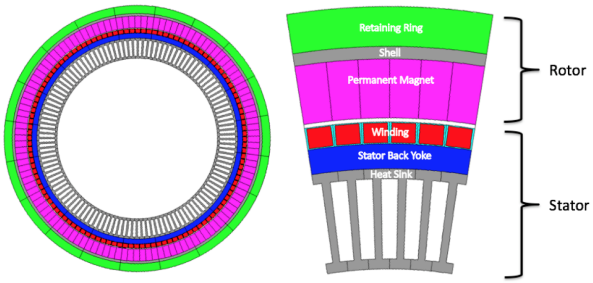

Figure 8. An Axial View of the High Frequency Motor

TABLE 2. KEY SPECS

Outer Diameter	12.926	in.
Active Length	8.8	in.
Retaining Ring Thickness	0.4	in.
Magnet Radial Depth	0.492	in.
Rotor Shell Thickness	0.125	in.
Airgap Length	0.04	in.
Winding Radial Depth	0.215	in.
Stator Yoke Thickness	0.249	in.
Heat Sink Depth	1.2	in.
Number of Poles	20	-
Rated Speed	18000	RPM

TABLE 3. LOSSES [KW]

Copper Losses	5.28	kW
Iron Losses	1.5	kW
Windage Losses	9-20	kW
Bearing Losses	1	kW
PM Losses	0.4	kW
Total Losses	17.2 - 28.2	kW
Efficiency	97.2-98.3	%

5. Conclusion & Future Work

This paper presented the design concept of a 1 MW, permanent magnet synchronous motor for aircraft application. The design utilizes high frequency, high pole-count, halbach arrays, and air-gap winding to minimize the use of heavy iron alloy. Furthermore, outer rotor topology is adopted to minimize effective air-gap. Preliminary optimization efforts and loss analysis suggests a 1 MW machine with power density of $> 13kW/kg$ and efficiency of $> 96\%$ is achievable.

Future work aims to further optimize the dimensions of the motor and explore lower speeds to further reduce mechanical risks. A prototype of rotor will be assembled and tested for vibration modes and expansion. Stator will also be assembled with coils to test thermal and electrical performance.

TABLE 4. WEIGHT BREAKDOWN

Retaining Ring	9.46	lb
Inconel Shell	35.23	lb
Permanent Magnet	48.74	lb
Copper	24.09	lb
Stator Yoke	19.51	lb
Ground Cylinder & Heat Sink	18.2	lb
Bearing retainers & rings	0.454	lb
Bearings	3.059	lb
Bolts	0.0324	lb
Total Weight	156.4	lb
Power Density	14	kw/kg

References

[1] "Vision 2050." (2011): IATA. Web. 22 Oct. 2015. http://www.iata.org/pressroom/facts_figures/documents/vision-2050.pdf.

[2] Felder, J.; Kim, H.; Brown, G.,"Turboelectric Distributed Propulsion Engine Cycle Analysis for Hybrid-Wing-Body Aircraft," 47th AIAA Aerospace Sciences Meeting including The New Horizons Forum and Aerospace Exposition, Jan 2009.

[3] Hathaway, M.D.; Rosario, R.; Madavan, N.K., "NASA Fixed Wing Project Propulsion Research and Technology Development Activities to Reduce Thrust Specific Energy Consumption," 49th AIAA/ASME/SAE/ASEE Joint Propulsion Conference, AIAA-2013-3605, 2013.

[4] Umans, Stephen D., and A. E. Fitzgerald. Fitzgerald & Kingsley's Electric Machinery. 7th ed. New York: McGraw-Hill Companies, 2014. Print.

[5] Zhu, Z.Q.; Howe, D., "Halbach permanent magnet machines and applications: a review," in Electric Power Applications, IEEE Proceedings - , vol.148, no.4, pp.299-308, Jul 2001

[6] Xu, T.; Sullivan, C.R., "Optimization of stranded-wire windings and comparison with litz wire on the basis of cost and loss." In Power Electronics Specialists Conference, 2004. PESC 04. 2004 IEEE 35th Annual, vol. 2, pp. 854-860. IEEE, 2004

[7] Chen Y.; Pillay, P., "An improved formula for lamination core loss calculations in machines operating with high frequency and high flux density excitation," Industry Applications Conference, 2002. 37th IAS Annual Meeting. Conference Record, vol.2, no., pp.759-766 vol.2, 13-18 Oct. 2002.

[8] Vrancik, J.E., "Prediction of windage power loss in alternators", NASA Technical Note, NASA TN D-4849, 1968.

[9] Childs, P., "Rotating cylinders annuli, and spheres", in Rotating Flow, Burlington, MA: Elsevier Inc., 2011.